energy&fuels

pubs.acs.org/EF Article

Potential of Light Oil and Condensates from Deep Source Rocks Revealed by the Pyrolysis of Type I/II Kerogens after Oil Generation and Expulsion

Qiang Wang, Wanglu Jia,* Chiling Yu, Jianzhong Song, Hui Zhang, Jinzhong Liu, and Ping'an Peng

Cite This: *Energy Fuels* 2020, 34, 9262−9274 Read Online

ACCESS | Metrics & More | Article Recommendations | Supporting Information

ABSTRACT: Light and condensable oils derived from mature kerogen and residual oil in deep source rocks have contributed strongly to a rapid increase in oil production. In this study, oil expulsion from kerogen and shale was simulated by selective solvent extraction (hexane/toluene, 9:1 v/v, instead of the commonly used dichloromethane) and by returning the extracts (so-called "oil a") back into a controlled mass of mature kerogen. The maturity intervals and potential of the light oil and condensates were investigated by analyzing the yields of different hydrocarbons from the subsequent pyrolysis of mature kerogen-"oil a" mixtures. The gas-to-oil ratio was used to constrain the maturity range for the light oil, condensate, and gas stages. The lowest equivalent vitrinite reflectance (EVR_o, 1.9−2.1%) for the gas stage was compatible with commonly accepted models. The EVR_o cutoff of 1.55−1.75% between light oil and condensate was higher than that in traditional models, although this depended primarily on the generality of the "condensate" definition. An EVR_o ranging between 1.35 and 1.55−1.75% was defined in this work as the "light oil/gas" substage within the commonly accepted condensate/wet gas stage. Moreover, yields of hydrocarbons from the cracking of "oil a" were distinctly affected by mature kerogen. This effect showed little difference on the yield of C_{6-14} hydrocarbons and C_{15+} hydrocarbons but notable difference for the gases between types I and II kerogens. The release of C_{6-14} hydrocarbons was promoted when the release of C_{15+} hydrocarbons was notably inhibited. Approximately linear relationships were established between maximum yields of liquid hydrocarbons and the carbon content of "oil a" (selective solvent extraction products) in the mixtures. This relationship was helpful in estimating both oil and total petroleum potential of deep source rocks that have undergone oil generation and expulsion, but it was dependent on the composition of the solvents used in extraction.

1. INTRODUCTION

Petroleum from relatively high maturity source rocks is gaining a greater importance. One example is the rapid growth of oil production in the U.S.A., which is primarily attributed to light and condensable oils produced from tight shales[1] within the interval 1.2−1.7% equivalent vitrinite reflectance (EVR_o) since 2010.[2] Conventional condensates from source rocks are also mainly formed at similar maturities (EVR_o 1.3−1.7%).[3−7] Notably large condensate fields have also been recently discovered in several basins in China, including the Tarim Basin.[8−10] Unconventional shale gas is produced mostly from postmature shales.[2,11,12] The tremendous progress in exploration for these resources has created a demand for assessment of the separate potentials of light oil, condensate/wet gas, and dry gas and not as whole oil or whole gas as before.

However, the names and classifications of the oil and gas stages at high maturity and overmaturity are diversely described in the literature, and definitions conflict at times. The condensate/wet gas stage refers to the interval between the principal oil formation stage and the dry gas zone.[13] "Condensates" commonly refers to oil with an API gravity greater than 45°, which is completely gaseous under reservoir conditions but condenses at the surface.[14,15] The condensates are defined as petroleum with a gas-to-oil ratio (GOR) greater than 5000 scf/bbl.[15] In contrast, light oil, the relatively highly matured product within the oil window of source rocks, is usually denoted as crude oil, with an API gravity of 35−45°,[14] although no consensus exists on the term for this range. For geochemists, light oil is mostly thought to be formed close to the end of the oil window with EVR_o < 1.35%, whereas the condensate is formed at the highly mature stage, with an EVR_o in the range 1.35−2.0%.[13,14,16] Therefore, petroleum geologists have defined those stages by using the oil density, the EVR_o of the source rock, and the physiochemical phase data for oils, among other factors. However, the detailed and systematic changes in chemical composition (e.g., C_1, C_{2-5}, C_{6-14}, and C_{15+} compounds) within those specific stages have rarely been reported in the literature and need further investigation.

The light oil, condensate/wet gas, and dry gas potential from kerogens depends on the type and maturities of kerogens, similar to normal oils. However, another important additional fact that we should consider is the effects of oil expulsion because the petroleum yields are mainly derived from cracking of mature kerogen and secondary cracking of residual oil,[13] thus losing most of the oil-generation potential. With

Received: February 20, 2020
Revised: May 19, 2020
Published: June 26, 2020

https://dx.doi.org/10.1021/acs.energyfuels.0c00553
Energy Fuels 2020, 34, 9262−9274

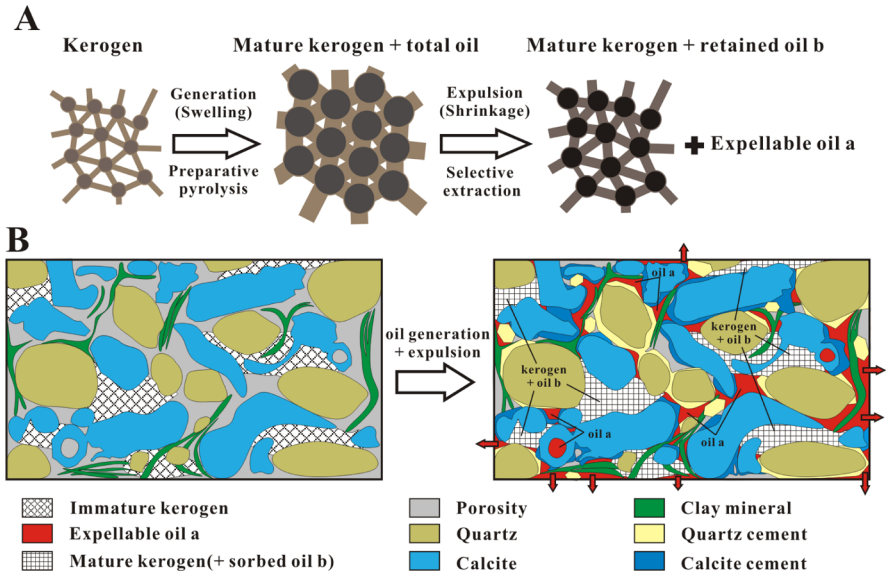

Figure 1. Schematics of oil expulsion related to (A) kerogen swelling and subsequent shrinkage and (B) migration of oil out of the shale layer (red arrows). Panel (A) is modified after Alcantar-Lopez,[26] and panel (B) is modified after Pommer and Milliken[27] and Loucks and Reed.[28]

consideration of oil expulsion, the yield and composition of gases from shale have been investigated in detail in many recent studies using pyrolysis experiments.[17−21] In contrast, the formation of hydrocarbons with respect to the maturity interval from the light oil to condensate/wet gas stages has been less studied, possibly because light hydrocarbons (the main fraction of light oil and condensate) are not easily manipulated in the laboratory. In addition, the preparation of suitable samples that have experienced oil expulsion to various degrees is crucial for this investigation.

First, we should determine the maturity of the sample when oil expulsion might occur. The maturity, which corresponds to the peak of normal oil generation, might be the best choice. Second, we must determine how to prepare the matured samples that represent different oil expulsion efficiencies (OEE). Extraction of artificially matured kerogen using strong solvents (such as chloroform), followed by addition of the extracts back into mature kerogen with different mass ratios, has been reported in the literature.[20] This process removes all polar compounds (resins and asphaltenes) that are preferentially retained in kerogen (Figure 1A), causing changes in hydrocarbon potential for matured kerogen. A kerogen-plus-sand system in a vessel has been used to study oil expulsion,[19] but it has the weakness of controlling OEE as well as the likelihood of thermal evaporation of oil from the kerogen to the sand.

Considering all of these factors, we chose a solvent assembly method (selective extraction), that is, *n*-hexane with minor amount of toluene rather than the normally used chloroform with excellent solubility, to extract the artificially matured samples. The material extracted by such a solvent, containing abundant hydrocarbons, might resemble the oil that can be easily expelled from the kerogen[22] into the inorganic pore system of the source rock (expellable "oil a", Figure 1) because nonpolar hexane is the major component of the solvent mixture. In contrast, the remaining "oil b" was thought to be tightly adsorbed or occluded by the kerogen structure and was thus nonexpellable, and it could coevolve with kerogen upon further thermal maturation. The adding back of extracts to the matured sample with different mass ratios formed a series of samples with different amounts of "oil a" expelled into the reservoir (Figure 1B). Although this method might not be perfect, it overcame many shortcomings of the previous methods.

Finally, we look to the catalytic effect of kerogen on residual oil cracking. Secondary cracking of retained oil into gases, as well as cracking of C_{2-5} to form methane, is promoted by type II kerogen in shale,[17,20] which is also true for cracking of oil in the presence of coal.[23,24] Close contact between the retained oil and kerogen might have significant effects on late gas generation.[17,20,23,25] We still do not know the possible effects of the interactions of oil and coexisting kerogen on the yields of liquid hydrocarbons (C_{6+}).

In this study, three types of low-maturity kerogens were first subjected to an oil-generation process with maturity up to the oil peak using a gold tube pyrolysis system. Matured samples experiencing oil expulsion were selected by using a solvent mixture of hexane and toluene (9:1 v/v), such that the group composition of the extracts was similar to that of normal oils (for details, see the Results section). Therefore, the extracts represented oil that can be expelled from the kerogen (expellable "oil a", Figure 1). Adding these extracts back into the kerogen at different mass ratios was used to obtain a series of samples with different OEE values. The hydrocarbons generated from these samples (gases and liquid hydrocarbons) were further simulated by pyrolysis in a confined system and compared in detail, thus supplying helpful data for evaluating the light oil and condensate potentials from deep source rocks.

2. SAMPLES AND EXPERIMENTS

Two outcrop samples of shale were collected for the concentration of kerogen: Eocene lacustrine Maoming shale (MM shale) from the southeastern Hainan Basin, China, and Ordovician marine Pingliang shale (PL shale) from the Ordos Basin, China. A sample of Jurassic Hongqing coal (HQ coal) from the Ordos Basin was used without pretreatment for subsequent pyrolysis because of its high total organic carbon (TOC) content. The shale samples were crushed to −200 mesh powder and demineralized by a normal digestion procedure using HCl and HF acids. Based on the locations

https://dx.doi.org/10.1021/acs.energyfuels.0c00553
Energy Fuels 2020, 34, 9262−9274

on the cross-plots of hydrogen index (HI) versus T_{max} (Figure 2a), MM kerogen, PL kerogen, and HQ coal were classified as

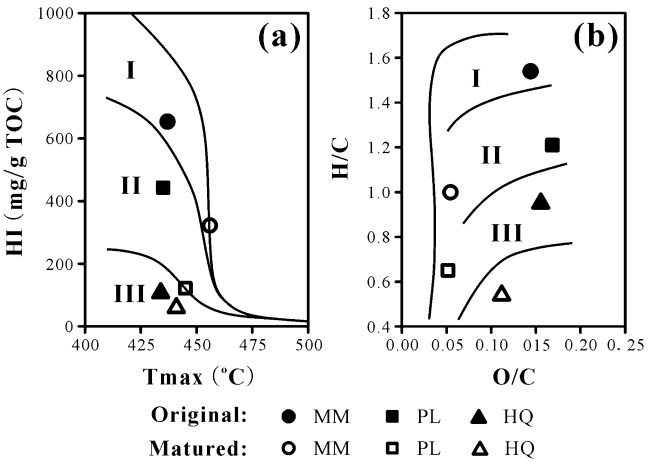

Figure 2. (a) HI vs T_{max}; (b) H/C vs O/C atomic ratio for original materials (solid symbols) and extracted with solvent mixture of hexane and toluene, mature kerogen, and coal samples (blank symbols).

types I, II, and III kerogen that are generally immature to marginally mature. The MM kerogen had a H/C atomic ratio of 1.54, almost identical to that of typical type I kerogen.[29−31]

The experiments in this study were composed of two major phases (Figure 3). The first phase involved the artificial

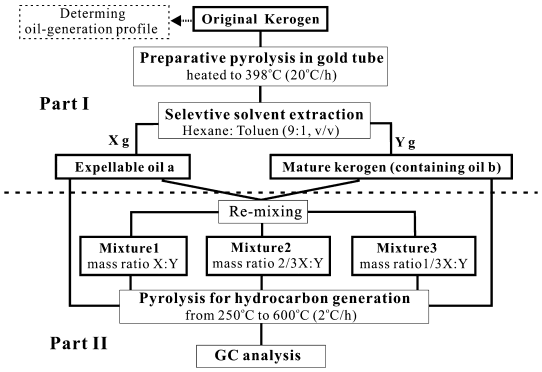

Figure 3. Flow chart of the experimental scheme of this study.

maturation of marginally mature kerogens to obtain uniformly matured kerogens and their evolved oils. Oil expulsion was simulated using selective solvent extraction, allowing a certain portion of total oil to be retained in the mature kerogen and chemical fractionation between the expellable "oil a" and kerogen-retained "oil b" (Figures 1 and 3). The second phase involved the pyrolysis of kerogen and "oil a" mixtures representing different oil-expulsion levels.

2.1. Simulation of Oil Expulsion from Kerogens. *2.1.1. Determination of the Oil-Generation Profiles.* An amount of 80−150 mg of each sample powder was placed in a gold tube (60 mm × 6 mm i.d.) and sealed in an argon atmosphere. The sealed tubes were placed in stainless steel vessels. A constant pressure of 50 MPa, supplied by a water pump, was exerted to compress the tubes. For each sample, six such vessels were placed in separate positions in a large cylindrical furnace and heated from room temperature to 100 °C in 5 h and subsequently to 460 °C at a rate of 20 °C/h. At each of six preset temperatures (364, 394, 414, 428, 442, and 458 °C; Figure 4a), one of the tubes was removed from the furnace and cooled in water as quickly as possible. These temperatures are routinely used in laboratory studies to cover the main oil generation stages in the pyrolysis of various types of kerogen. The tube was quickly cut open, and the sample was ultrasonically extracted by using dichloromethane. The extracted material was filtered, concentrated, and weighed. As shown in Figure 4a, the yields of total oil peaked at 414 °C for MM kerogen and at 394 °C for PL kerogen and HQ coal. For convenience of comparison at a constant maturity level and to avoid severe secondary oil cracking released from type II kerogen, 398 °C was chosen as the temperature for subsequent preparative pyrolysis.

2.1.2. Preparative Pyrolysis and Selective Solvent Extraction. Relatively large samples were placed in larger gold tubes (100 mm × 10 mm i.d.) and pyrolyzed to 398 °C (see Subsection 2.1.1) to enable sufficient quantities of "oil a" and mature kerogen to be obtained. After pyrolysis, the gold tubes were cut open and subjected to selective Soxhlet extraction using a solvent mixture of *n*-hexane and toluene (9:1 v/v, part I in Figure 3). These extracts were referred to as expellable "oil a" (Figures 1 and 3). The "oil a" and remaining matured kerogens after extraction were separately recovered, dried, and weighed. A portion of each matured kerogen was extracted again using the conventional solvent mixture of dichloromethane and methanol (25:2 v/v) to assess the amount of "oil b" retained in the kerogen (Figure 1). The "oil b" and residual solids were also recovered, dried, and weighed. The fractional compositions of "oil a" and "oil b" were determined by column chromatography after precipitation of

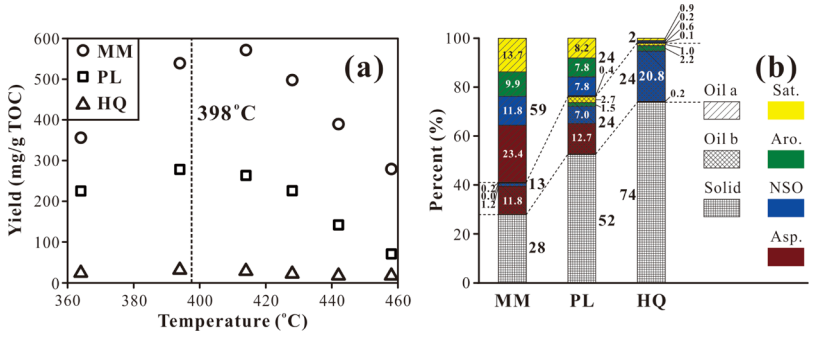

Figure 4. (a) Total oil-yield profiles for three sampled materials; (b) relative amounts (wt %) of organic fractions in "oil a" and mature kerogen ("oil b" + solids) for the three samples after preparative pyrolysis at 398 °C.

https://dx.doi.org/10.1021/acs.energyfuels.0c00553
Energy Fuels 2020, 34, 9262−9274

Table 1. Geochemical Data of Two Kerogen and Coal Samples before (Original) and after (Matured) Preparative Pyrolysis[a]

S	type	VR_o (%)	S_1 (mg/g)	S_2 (mg/g)	S_3 (mg/g)	T_{max} (°C)	HI (mg/g)	OI (mg/g)	TOC[c] (%)	H/C	O/C	$\delta^{13}C$ (‰)
MM	original	0.45	7.24	402.01	10.84	437	653.7	17.4	61.50	1.54	0.14	−20.8
	matured	n.d.	5.33	203.41	2.32	456	321.6	4.4	63.24	1.00	0.05	−20.5
PL	original	0.76[b]	21.89	303.23	30.77	435	442.0	44.6	68.60	1.21	0.17	−30.8
	matured	n.d.	13.16	95.91	4.12	445	120.8	5.1	79.38	0.65	0.05	−30.7
HQ	original	0.64	0.43	83.27	6.83	434	107.5	8.6	77.44	0.95	0.16	−23.4
	matured	n.d.	0.22	50.64	1.74	441	60.2	7.2	84.09	0.54	0.11	−23.3

[a]Mature kerogen was measured after extraction using the hexane/toluene (9:1, v/v) solvent mixture. [b]Reflectance of solid bitumen was measured and reported because of a lack of vitrinite in the Ordovician shale. [c]TOC content was determined using an elemental analyzer.

the asphaltene fraction by adding an excess of hexane to the extracts. Saturated hydrocarbons, aromatic hydrocarbons, and resins were eluted with hexane, a mixture of hexane and chloromethane (3:2 v/v), and methanol. Each fraction was concentrated, dried, and weighed.

2.2. Pyrolysis of Mature Kerogens with Different OEE Values. *2.2.1. Simulation of Oil Expulsion from Shale at Different Levels.* The migration out of the shale layer of "oil a", infilling the various types of inorganic pores (Figure 1B), was not easily quantified[32,33] because of several influencing factors (e.g., internal fluid pressure) related to the total oil potential, sedimentation characteristics, and structures of inorganic pores. To simplify this process, "oil a" was mixed with mature kerogen at different mass ratios (Figure 3, part II). Each matured kerogen sample was divided into four equal portions and subsequently mixed with "oil a" solvent in the ratios 1 WR, 2/3 WR, and 1/3 WR, where WR refers to the original mass ratio of "oil a"-to-mature kerogen (X/Y in Figure 3, part I). The mixtures were homogenized by successive procedures of thorough stirring, solvent evaporation, and grinding in an agate mortar.

2.2.2. Simulation of Hydrocarbon Generation of Kerogens. The mixtures, mature kerogen (containing "oil b"), and "oil a" were initially heated from room temperature to 250 °C in 10 h and subsequently pyrolyzed to 600 °C at a rate of 2 °C/h while subjected to a pressure of 50 MPa. The procedure described below for the analysis of the generated gases was previously reported.[19] Typically, the gold tube was carefully placed in a customized vacuum line connected to an Agilent 6890N gas chromatograph (GC) modified by Wasson-ECE Instrumentation. The tube was pierced under vacuum using a steel needle to release the gas products, which were automatically introduced into the GC through a connecting valve, and their molecular compositions were determined. The external standard method was used in quantification, and the analytical errors were usually <0.5%.

Another parallel gold tube was used in the analysis of C_{6+} compounds to avoid possible loss of light hydrocarbons during the gas analysis. The tube was first immersed in liquid nitrogen for 1 min, cut open with scissors, and immediately placed in an 8 mL vial containing 4 mL of chloromethane and an internal standard (C_{24} deuterated *n*-alkane) for quantification. The vial was sealed with a cap, and its contents were ultrasonically extracted. The solution of total extracts was analyzed on an Agilent 7890 GC equipped with a flame ionization detector to determine the amounts of C_{6+} compounds. The GC-undetectable polar compounds (resins and asphaltenes) were not quantified.

During the extraction of "oil a" and successive mixing with mature kerogen, a certain amount of evaporative loss of light hydrocarbons (C_{6-14}) in "oil a" could not be avoided. This loss was expected to result in a certain decrease of gas yields from "oil a" and related mixtures. The mass loss of light hydrocarbons during the oil extraction process was believed to be less than 5% of the total oil (C_{6+}) yields after comparing the GC-detected oil compounds from kerogen MM directly extracted from the gold tube and "oil a" after concentration. The process of mixing mature kerogen and "oil a" should not have significantly influenced the mass loss of C_{6-14} compounds because most of the evaporative loss occurred during the extraction of "oil a". Therefore, the obtained gas potentials of "oil a" and the mixtures of "oil a" with mature kerogen were slightly underestimated in this study.

3. RESULTS

3.1. Compositional Characteristics. *3.1.1. Mature Kerogens with Retained "Oil b".* Types I and II kerogens exhibited much greater changes in composition than coal (Figure 2; Table 1) after pyrolysis and selective solvent extraction. The HI values of the MM and PL kerogens decreased by 332 and 321 mg/g TOC, respectively, but the HQ coal showed a notably small decrease (47 mg/g TOC, Figure 2; Table 1). However, the kerogen and coal samples all displayed an obvious decrease in the H/C atomic ratio (between 0.41 and 0.56), indicating that the loss of hydrogen was larger than the loss of carbon in the matured samples compared with the original unprocessed materials (Table 1). This observation is consistent with previously reported evolution trends for atomic ratios and Rock-Eval indices defined for three distinct types of kerogen.[13,34] The two mature kerogens still have hydrocarbon-generation potentials (HI = 322 and 121 mg/g TOC) and free hydrocarbons (S_1/TOC values of 8.4 and 16.6 mg/g TOC, where S_1 is the amount of free hydrocarbons in the sample).

3.1.2. Expellable "Oil a" and Retained "Oil b". The mass percentages of total oil (expellable "oil a" plus retained "oil b") in the initial samples were 72, 48, and 26% for the type I kerogen MM, type II kerogen PL, and type III coal HQ, respectively (Figure 4b), consistent with a decreasing oil potential for the three samples (Figure 2). Interestingly, expellable "oil a" also decreased from type I kerogen MM (59%) to type II kerogen PL (24%) and to coal sample HQ (2%), as shown in Figure 4b. In contrast, "oil b" retained in the mature kerogens varied in the order of type I kerogen MM (13%) < type II kerogen PL (24%) = coal sample HQ (24%). Considering the retained "oil b", the OEE values for three types of kerogen were observed at greatly different levels (Figure 4), as follows. For mixture 1, the OEE value was 0% because all of "oil a" had been added back into the mature kerogen. For type I kerogen MM, mixtures 2 and 3 and the mature kerogen had OEE values of 27, 55, and 82%, respectively, and in contrast, these values were 17, 33, and

https://dx.doi.org/10.1021/acs.energyfuels.0c00553
Energy Fuels 2020, 34, 9262−9274

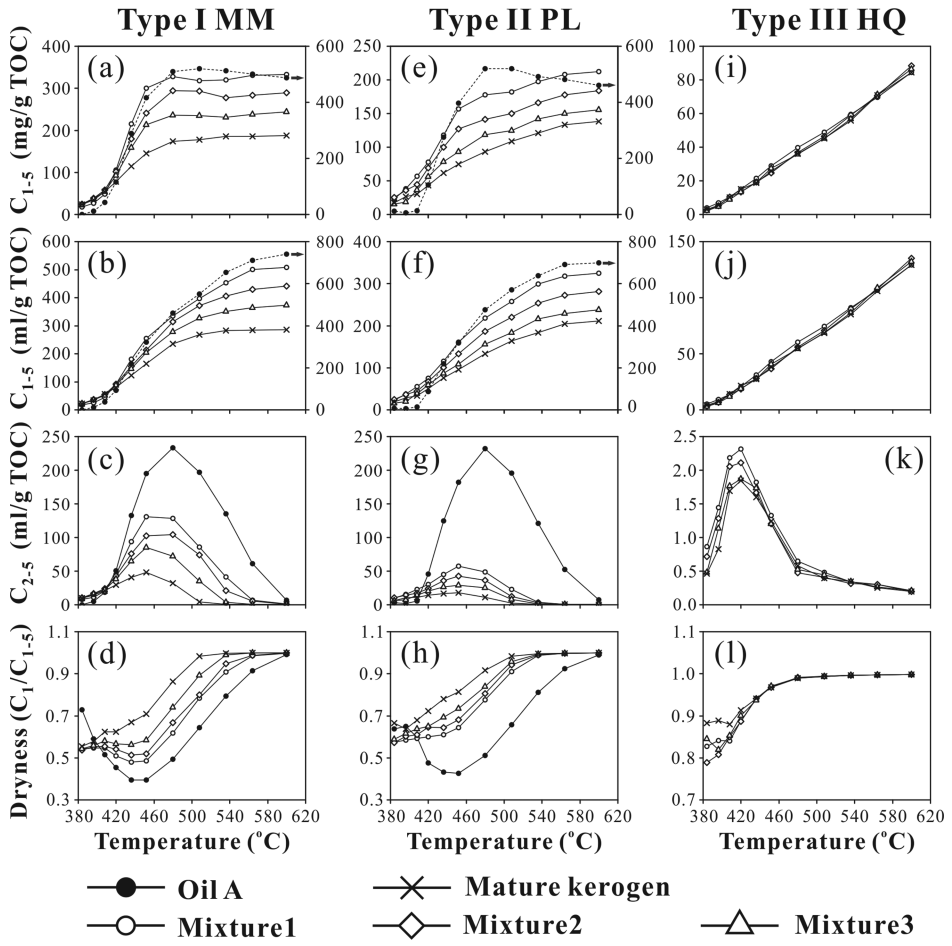

Figure 5. Yields and dryness of gases released from "oil a" and kerogen series: (a–d) for type I kerogen MM; (e–h) for type II kerogen PL; and (i–l) for type III coal HQ. For convenience of illustration, total gas yield of "oil a" is displayed on the right-hand *y*-axis, as shown by the arrows in panels (a,b,e,f).

50%, respectively, for type II kerogen PL. The OEE of the coal samples ranged from 2 to 7%.

Upon selective solvent extraction, chemical fractionation of the oil from the three types of kerogen also displayed distinct characteristics. For type I kerogen MM, nearly all of the hydrocarbons (saturated and aromatic compounds) and resins appeared in "oil a" but were absent in "oil b". Approximately two-thirds of total asphaltenes were detected in "oil a", and the remainder were found in "oil b". For type II kerogen PL, approximately 80% of total hydrocarbons and 50% of total resins were found in "oil a", and nearly all of the asphaltenes remained in "oil b". For type III coal HQ, only 8% of total pyrolyzates was extracted as "oil a", with "oil b" occurring primarily as resins and a notably small amount of hydrocarbons (<15% of "oil b"). These observations are consistent with the model illustrating the effects of sorption–fractionation on the expelled oil quality for various types of kerogen (Figure 11 in Pepper and Corvi).[35] In that study, for kerogen with HI of 1000, all of the hydrocarbons and resins and most of the asphaltenes were expelled. For kerogens with medium HI, more resins and asphaltenes were retained, and for kerogen with low HI, most of the generated hydrocarbons and nearly all of the polar compounds (resins and asphaltenes) were retained.

3.2. Yields of Gases. Because of the low yields of total expelled oil from mature HQ coal, the yields of gases varied minimally with increasing OEE values. In contrast, the MM and PL kerogens both varied significantly with changing OEE but to different extents. The curves of total gas generation are usually illustrated both in volume and in mass for oil cracking because volume-generation curves might indicate secondary cracking of C_{2-5} gases into methane and mass-generation curves might indicate cracking of oil (C_{6+}) into gas.[19,36−38] When the peak of C_{2-5} generation was reached at 452 °C (Figure 5c,g), the weight of total gas (C_{1-5}) began to decrease rather slowly (as shown in Figure 5a,e). This observation suggested little contribution to total gas from C_{6+} cracking and suggested that the weight loss of total gas was associated with the formation of pyrobitumen during secondary cracking of C_{2-5} to methane.[36−38] However, a decreasing weight of total gas was seldom observed for the pyrolysis of kerogens with relatively low oil potential (type II kerogens in Figure 5e compared with type I kerogens in Figure 5a),[39] which supported the suggestion of a relatively small contribution from oil cracking to total gas. In contrast, the total volumetric gas yield during oil cracking continued to increase (Figure 5b,f) beyond the C_{2-5} generation peak (Figure 5c,g) because further cracking of C_{2-5} into methane leads to substantial volume expansion. Because of the smaller contribution from oil cracking, the dryness of the yielded gases increased with increasing OEE for kerogens MM and PL (Figure 5d,h).

https://dx.doi.org/10.1021/acs.energyfuels.0c00553
Energy Fuels 2020, 34, 9262−9274

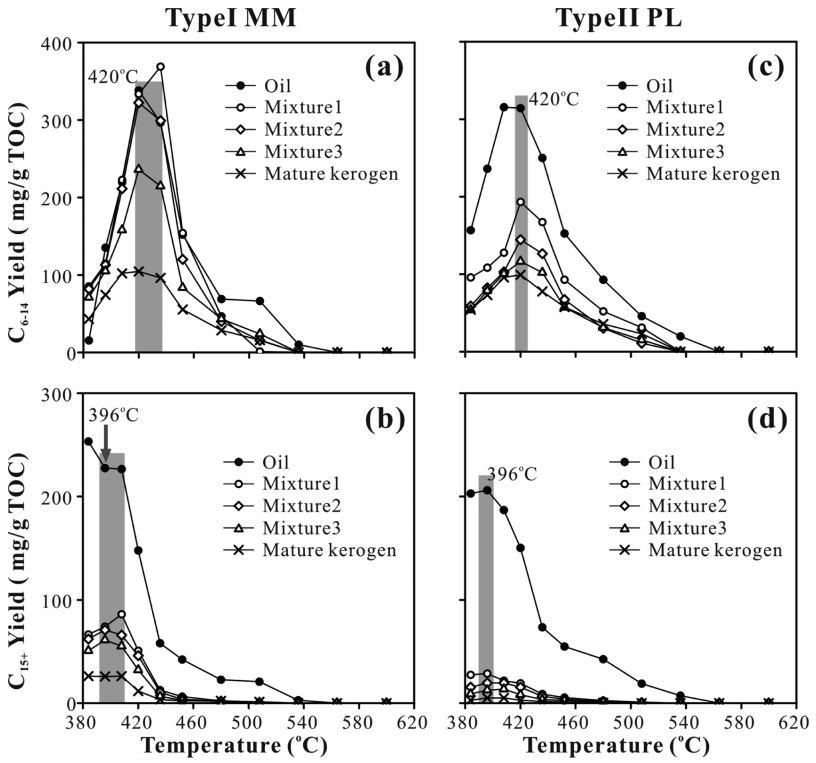

Figure 6. Yields of C_{6-14} and C_{15+} hydrocarbons from "oil a" mixture series and mature kerogen: (a,b) type II kerogen MM and (c,d) type I kerogen PL.

Notably, the HQ coal showed a roughly linear increase in the total gas yield at elevated temperatures (Figure 5i,g).

3.3. Yields of C_{6+} Hydrocarbon. Generally, the change in the C_{6+} hydrocarbon yield curves (Figure 6) was not as smooth as those of gas yield (Figure 5), probably resulting from the off-line analytical procedures applied for C_{6+} hydrocarbons. In addition, the yields of C_{6+} compounds from coal HQ were negligible and were not detected by the GC analysis.

3.3.1. C_{6-14} Hydrocarbons. Although greatly affected by oil expulsion, the yield profiles of C_{6-14} hydrocarbons of both kerogen series displayed typical single peak shapes (Figure 6a,c). This observation suggested that the temperature settings used in the preparation and subsequent pyrolysis covered both the main generation and cracking stages of C_{6-14} hydrocarbons, the principal fraction of light oil and condensates. The pyrolysis temperature at which the generation peak was observed was approximately 420 °C (Figure 6a,c), notably lower than that for C_{2-5} gases (452 °C, Figure 5c,g). The maximum yield of C_{6-14} hydrocarbons from type I mature kerogen MM was notably close to that from type II mature kerogen PL (~100 mg/g TOC, Figure 6a,c). The maximum yield of C_{6-14} hydrocarbons from "oil a" in kerogen MM (~340 mg/g TOC, Figure 6a) slightly exceeded that from kerogen PL (~320 mg/g TOC, Figure 6c). In contrast, the C_{6-14} hydrocarbon yield increased with decreasing OEE (from mature kerogen to mixture 1) to much greater extent for MM samples (Figure 6a) than for PL samples (Figure 6c). In addition, the maximum C_{6-14} hydrocarbon yield of mixtures 1 and 2 of kerogen MM (OEE 0, 27%) was comparable to that of "oil a" (Figure 6a). However, mixture 1 of kerogen PL had a maximum C_{6-14} hydrocarbon yield (~190 mg/g TOC) that was only approximately 60% of that of "oil a" (Figure 6c).

3.3.2. C_{15+} Hydrocarbons. Yields of C_{15+} hydrocarbons at first remained roughly constant within the relatively low temperature interval of 384−408 °C and subsequently showed an overall decreasing trend with elevated temperatures for both "oil a" mature kerogens and their mixtures (Figure 6b,d). This observation suggested almost complete generation of heavy hydrocarbons after the preparative pyrolysis of the original kerogens (Figures 3 and 4a). Oil pyrolysis in a confined system[40] also displayed a progressively decreasing trend for C_{15+} hydrocarbons. In the Hill et al.[40] study, C_{15+} hydrocarbons included not only GC-detectable compounds but also resins and asphaltenes quantified by weight. However, "oil a" from kerogens MM and PL both contain a notable content of polar fractions, that is, resins and asphaltenes (Figure 4b), which are a source of hydrocarbons.[41,42] A comparison by Bowden et al.[42] between catalytic hydropyrolysis of resins and asphaltenes and solvent-extracted product from organically enriched rocks revealed much lower yields of resins than asphaltenes. Therefore, the generation and secondary cracking of C_{15+} hydrocarbons should reach a balance at relatively low pyrolysis temperatures for both "oil a" and the mature kerogen series.

The maximum yield of C_{15+} hydrocarbons of "oil a" from kerogen MM (~250 mg/g TOC, Figure 5b) was larger than that of "oil a" from kerogen PL (~200 mg/g TOC, Figure 5d). In contrast, this yield from type I mature kerogen MM (~86 mg/g TOC) was much greater than that from type II mature kerogen PL (~29 mg/g TOC). Compared with C_{6-14} hydrocarbons (Figure 6a,c), the maximum yield of the corresponding C_{15+} hydrocarbons for both mixture series was astoundingly lower (Figure 6b,d), probably because the GC-nondetectable fractions (mainly resins and asphaltenes) were not included among the C_{15+} hydrocarbons present.

https://dx.doi.org/10.1021/acs.energyfuels.0c00553
Energy Fuels 2020, 34, 9262−9274

Table 2. EVR_o and Easy% R_o Values Determined at Corresponding Pyrolysis Temperature Points

Temp. (°C)	384	396	408	420	436	452	480	508	536	564	600
EVR_o (%)	1.18	1.27	1.36	1.45	1.61	1.85	2.08	2.23	2.51	2.95	3.59
Easy% R_o (%)	1.08	1.22	1.35	1.52	1.75	2.02	2.52	3.07	3.6	4.04	4.44

4. DISCUSSION

The primary sources of petroleum in deep source rocks are mature kerogen and residual oil. Many studies have suggested a catalytic effect of the kerogen on secondary cracking of residual oil.[17,20,23,24,43,44] Promotion of oil cracking into gas by kerogen in shales has long been observed[17,44] and could be a crucial factor controlling gas generation from shale.[17] A recent study has suggested a delay in gas yield within the C_{2-5} generation stage and an accelerated subsequent C_{2-5} cracking into methane.[20] More importantly, that research further demonstrated that no change occurred in the total-gas potential (maximal yield) for oil cracking, either with or without the presence of a type II kerogen.

Therefore, the following sections first focused on the influence of oil expulsion on the thermal intervals for different types of petroleum resources based on variations in the relative amounts of oil and gas. The effects of kerogen on oil cracking with respect to the yields of individual hydrocarbon fractions (C_1, C_{2-5}, C_{6-14}, and C_{15+}) and the relationships between the oil and total petroleum potentials and the oil-expulsion levels were also evaluated on that basis.

4.1. Thermal Maturity Ranges for Light Oil and Condensates. In this study, the EVR_o scale was adopted rather than temperature under geological conditions because only four or five data points could be used to constrain the profiles of liquid hydrocarbon generation (Figure 6). This process was not sufficient to construct the conversion curve used in kinetic analysis. With respect to the limits for the light oil and condensate substages, the GOR was applied based on the existing common definitions and criteria.[15,45]

4.1.1. EVR_o Scale for the Current Experiment Conditions. The Easy% R_o model, originally developed by Sweeney and Burnham,[46] has occasionally been used in simulation experiments with different original materials.[19,20,40] This approach can be convenient for direct comparison among different pyrolysis systems or different types of OM but might not be sufficiently accurate for specific pyrolysis conditions. In addition, VR_o measurement is not an ideal choice for type I/II kerogens because of the relatively small amounts of vitrinites available. In this work, previously obtained kinetic parameters were used in EVR_o conversion of one vitrinite isolate[47] pyrolyzed together with type II kerogen under the same pyrolysis system and conditions used in this study. The EVR_o and Easy% R_o values at the sampling temperatures are listed and compared in Table 2.

4.1.2. Influences of Oil Expulsion. At EVR_o values <1.4% for the two samples, the GOR of the mature kerogen and related mixtures either increased only slightly or showed little change (Figure 7). Oil expulsion more evidently affected the GOR of the MM sample series (Figure 7a) than the PL sample series (Figure 7b), that is, it increased notably with the increasing oil-expulsion level, from ~500 scf/bbl for mixture 1 to ~2000 scf/bbl for the mature kerogen (Figure 7a). In contrast, the GOR of the PL samples showed less variation, mainly within the range 1000−2000 scf/bbl (Figure 7b). Within this maturity range (EVR_o < 1.4%), the GOR values of two "oil a" samples were significantly lower than the GOR of

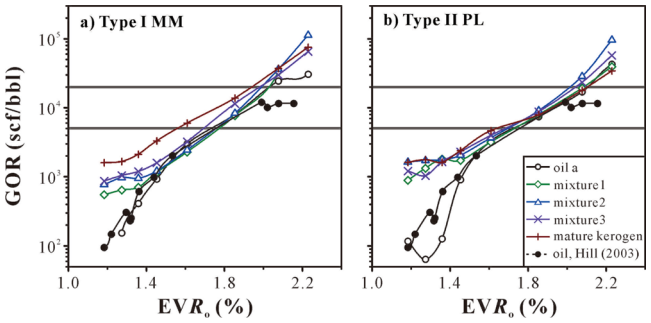

Figure 7. Variations in GOR with EVR_o values for (a) MM samples and (b) PL samples.

the kerogen series but began to converge toward the kerogen values (Figure 7). In addition, the GOR values of "oil a" from type I kerogen MM were almost identical to those reported previously by Hill et al.[40] In contrast, a relatively large difference in the GOR was noticeable between "oil a" from type II kerogen PL and the Hill et al.[40] value. The difference might have been due to evaporation loss during the separation and loading processes of the pyrolysis because the solvent applied for "oil a" had to be removed.

For EVR_o > 1.4%, the GOR of the kerogens and their mixtures with "oil a" increased rapidly, and a relatively small difference was observed between the mixtures and "oil a" itself, as well as the previously reported oil (Figure 7). It was still evident that the GORs of mature kerogen MM were notably larger than those of the corresponding mixtures (Figure 7a). In contrast, the type II kerogen PL and its mixtures showed rather similar GORs (Figure 7b). The noted GOR variations for EVR_o > 1.4% were highly important because the condensate or wet gas stage commonly started at this point and persisted up to an EVR_o of 2.0% in commonly accepted petroleum evolution models.[13,14,16] In addition, the GOR was also critical for the difference between oil and condensates in conventional reservoirs.[15] A critical GOR of 5000 scf/bbl has been suggested to represent the upper limit for the presence of a separate oil phase in a reservoir. This observation is consistent with the uppermost GOR of "oil" produced in Oklahoma.[45] When the GOR exceeded this value, the oil components (C_{6+}) were completely dissolved in gases in reservoir conditions and thus released condensable oil and gas at the ground level. For type I kerogen MM and its mixtures, a GOR of 5000 scf/bbl requires an EVR_o of 1.55−1.75%, which increased slightly with decreasing oil-expulsion levels (Figure 7a). In contrast, type II kerogen PL and its mixtures displayed a relatively narrow EVR_o range of 1.6−1.7% (Figure 7b). Therefore, these lower limits of EVR_o for the condensate (wet gas) stage defined by this approach were higher than the normally accepted EVR_o (~1.35%).[13,14,16]

The uppermost GOR of 20,000 scf/bbl for "oil and gas" suggested by Boyd[45] was adopted as the upper EVR_o limit for the condensate stage. When the GOR exceeded this value, only gas was produced. This ratio corresponded to the narrow EVR_o ranges of 1.9−2.0% for type I kerogen MM and its mixtures (Figure 7a) and 2.0−2.1% for type II kerogen PL and its

https://dx.doi.org/10.1021/acs.energyfuels.0c00553
Energy Fuels 2020, 34, 9262−9274

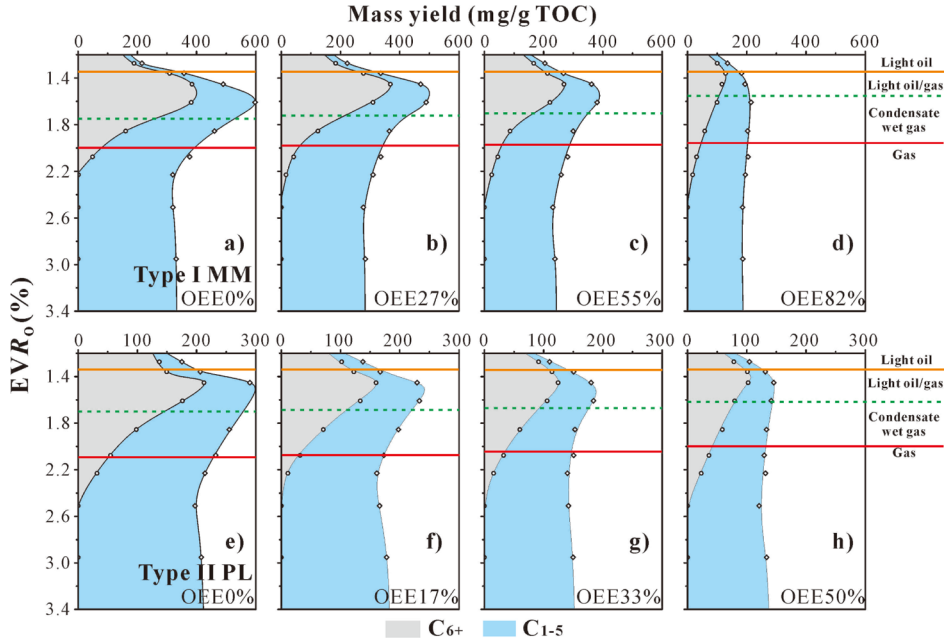

Figure 8. Variations in yields of gas and C_{6+} with increasing EVR_o for mature kerogens at different oil-expulsion levels: (a–d) type I MM and (e–h) type II PL.

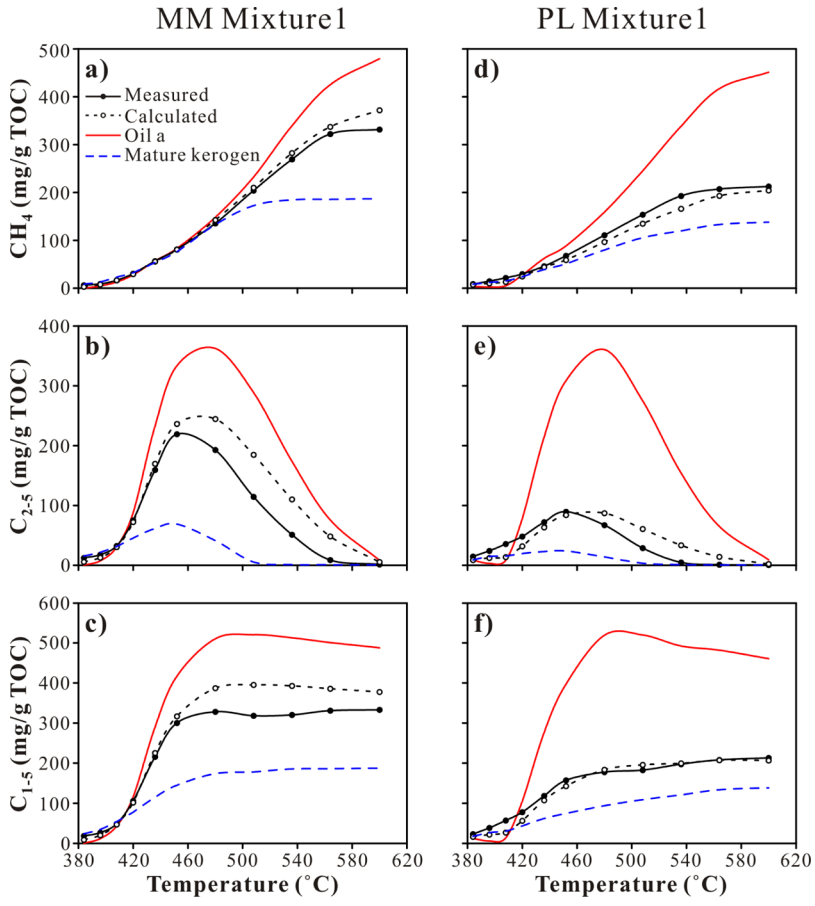

Figure 9. Comparisons of measured and calculated gas yields for oil–kerogen mixture 1 of type I MM and type II PL samples. The measured gas yields of "oil a" (red line) and mature kerogen (blue dashed line) are also shown for ease of discussion.

mixtures (Figure 7b). As such, the two EVR_o ranges agreed well with each other for type I and II kerogens with different oil-expulsion levels.

In summary, the lower EVR_o limit determined for the gas stage in type I and II kerogens (1.9–2.1%) was consistent with commonly accepted models ($VR_o \sim 2.0\%$).[13,14,16] The

https://dx.doi.org/10.1021/acs.energyfuels.0c00553
Energy Fuels 2020, 34, 9262–9274

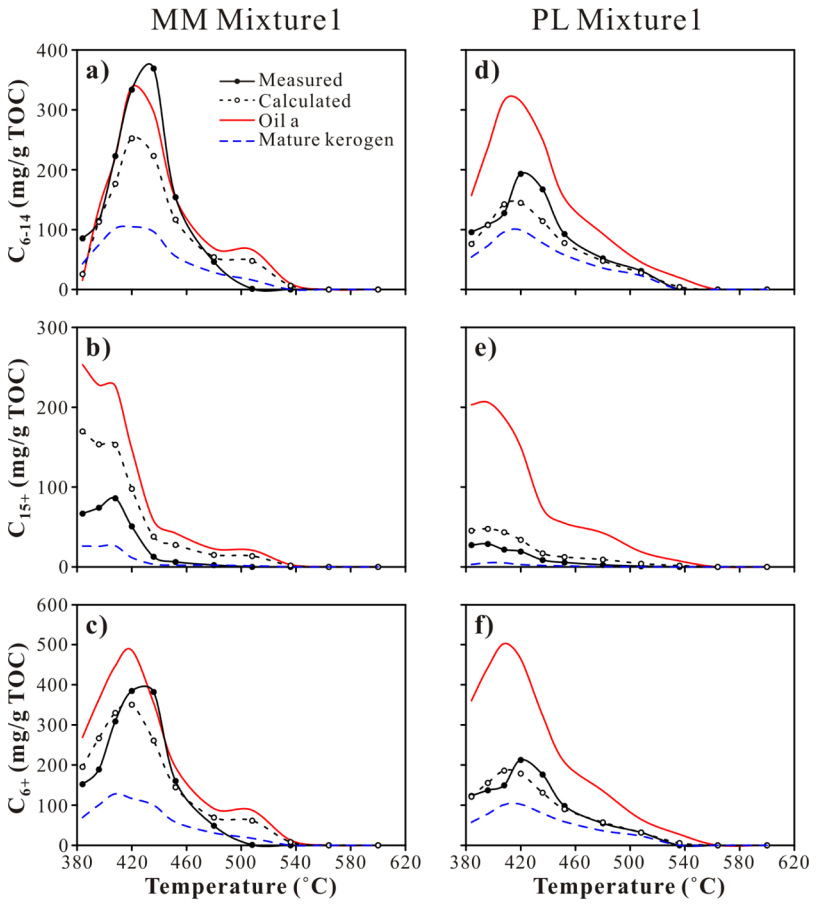

Figure 10. Comparisons of measured and calculated C_{6+} yields for oil−kerogen mixture 1 of type I MM and type II PL samples. For convenience of discussion, the measured gas yields of "oil a" (red line) and mature kerogen (blue dashed line) are also shown.

difference in the EVR_o cutoff between the oil and condensate stages was mainly related to the definition of condensate. In general, one could imagine that even if both liquid oil and gas were to exist under reservoir conditions, they could still exhibit condensable properties once transported to the ground level. It seemed that the relatively low limit ($EVR_o \sim 1.35\%$) for the condensate stage in commonly accepted models might have been defined as the point at which the petroleum begins to show a rapid increase in GOR (Figure 7). In addition, it has been shown that for Woodford Shale from Oklahoma, the production of condensates originated mostly from shale with maturity no more than R_o 1.7%.[2] However, our observation corresponded to a rigorous definition of the "condensate" based on GOR ratios (Figure 7). Nevertheless, C_{6+} hydrocarbons showed significant cracking from this point (as indicated in Figure 8), which might suggest notably low production of condensable oil in practice. Therefore, we suggest an EVR_o range from 1.35% (relatively low GOR) to 1.55−1.75% (disappearance of separate oil phase) as the "light oil and gas" substage, together with a more advanced maturity range (EVR_o up to 1.9−2.1%, Figure 8) as the "condensate/wet gas" stage. Petroleum produced from mature kerogens with EVR_o smaller than 1.35%, and possibly as low as 1.0%, could be classified as "light oil".

At the lower limits of "gas", "condensate/wet gas", and "light oil/gas" (also the upper limit of "light oil") substages, the mass percentages of gases were approximately 72−81, 48−64, and 14−30%, with C_{2-5} percentages of 12−52, 18−37, and 9−17% and CH_4 percentages of 25−60, 13−38, and 5−13%, respectively. The relatively large variations of the CH_4 and C_{2-5} percentages were related to the oil content of kerogen. Normally, kerogen with more oil could produce hydrocarbons with more C_{2-5} gases. However, the total gas (C_{1-5}) content at each substage boundary was relatively stable.

4.2. Effects of Mature Kerogen on Hydrocarbon Fractions Generated by Oil Cracking. Following the procedure suggested in previous studies,[20,23] the measured and calculated hydrocarbon yields were compared for the oil−kerogen mixes. The theoretical hydrocarbon yields of the oil−kerogen mixes ($Y_{(O+K)}$ in mg/g of TOC, without considering any interactions between oil and kerogen) were calculated from the hydrocarbon yields of the oil and mature kerogen

$$Y_{(O+K)} = (Y_{(O)} \times M_{(O)} \times C_{(O)} + Y_{(K)} \times M_{(K)} \times C_{(K)}) / ((M_{(O)} + M_{(K)}) \times C_{(O+K)}) \quad (1)$$

where $Y_{(O)}$ and $Y_{(K)}$ are the hydrocarbon yields of oil and matured kerogen (mg/g TOC), respectively; $M_{(O)}$ and $M_{(K)}$ are the weights of oil and matured kerogen (g), respectively; $C_{(O)}$ and $C_{(K)}$ are the TOC contents of the oil and matured kerogen, respectively; and $C_{(O+K)}$ is the TOC content of the mixtures of "oil a" with matured kerogen at the given mass ratios (Figure 3). The measured TOC contents of oil, matured kerogen, and their mixtures are listed in the Supporting Information file, together with their hydrocarbon yields.

4.2.1. Yields of Gases. The typical comparisons of calculated and measured gas yields for mixture 1 (i.e., when all generated "oil a" was added back to the mature kerogen) are

https://dx.doi.org/10.1021/acs.energyfuels.0c00553
Energy Fuels 2020, 34, 9262−9274

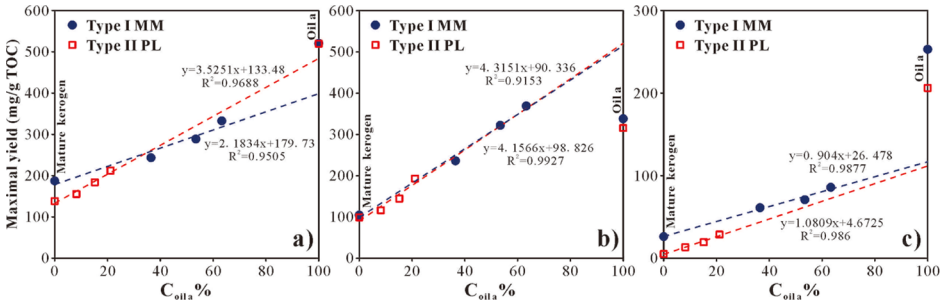

Figure 11. Relationships between $C_{oil\ a}$ % and maximum yields of (a) C_{1-5}, (b) C_{6-14}, and (c) C_{15+} fractions. Sample points plotted on the left- and right-hand *y*-axes represent mature kerogen and "oil a", respectively, and points lying between them represent their mixtures (linear regressions are determined for the MM and PL samples separately, excluding "oil a" data).

illustrated in Figure 9. The different influences of mature kerogen on the gas yielded by oil cracking can be observed for type I MM and type II PL mixtures. At relatively low temperatures (380−436 °C), the measured yields of individual gases (C_1 and C_{2-5}, Figure 9a,b) and of total gases (C_{1-5}, Figure 9c) did not differ from the calculated yields, suggesting a negligible influence of type I mature kerogen MM on oil cracking into gas. When the pyrolysis temperature increased to 452 °C, the measured yields of C_{2-5} gases and total gases increased more slowly than the calculated yields, and the maximum measured C_{2-5} gas yield was considerably lower than the calculated yield (Figure 9b,c) throughout the entire cracking stage for C_{2-5} gases (480 °C and above). In contrast, this difference was observed for methane up to relatively high temperatures (508 °C and above, Figure 9a). This overall trend suggested that type I mature kerogen had an inhibiting effect on the late cracking of oil into C_{2-5} gases (Figure 7b), and the pyrobitumen formed during the cracking of kerogen and "oil a" might also reduce the generation of C_{2-5} gases, resulting in lower yields of both methane (from cracking of C_{2-5} gases) and total gases than the calculated yields (Figure 9a,c).

In the case of type II PL kerogen, early promotion of oil cracking into C_{2-5} gases (380−420 °C, Figure 9e) was evident and was also clear in the case of total gases (Figure 9f). At higher pyrolysis temperatures (436−452 °C), the difference was less pronounced. Above 452 °C, the measured yield of C_{2-5} gases was significantly less than that calculated (Figure 9e), but the measured methane yields became noticeably larger than the calculated values (Figure 9d). The measured yields of total gases were consistent with the calculated yields within this interval (Figure 9f). Considering that the measured maximal gas yields of type II kerogen approximately agreed with the calculated yields, these findings suggested that type II kerogen promoted secondary cracking of C_{2-5} gases into methane rather than inhibiting C_{2-5} generation, as was found for type I MM kerogen (Figure 9a−c). Hence, type II kerogen PL not only promoted oil cracking into gases but also caused further cracking of C_{2-5} gases into methane, producing drier gases than those calculated for simple mixing of kerogen and oil. This observation agrees well with previous reports that kerogen lowers the thermal maturity required for appreciable gas generation from oil cracking in source rocks.[17,44]

4.2.2. Yields of C_{6+} Hydrocarbons. Many similarities were observed in the variations in the yields of C_{6+} hydrocarbons generated by the two types of kerogen−oil mixtures (Figure 10). Generally, the measured yields for C_{15+} hydrocarbons were much smaller than calculated yields across the entire temperature range (type I MM, Figure 8b and type II PL, Figure 10e). In contrast, the measured and calculated yields of C_{6-14} hydrocarbons were reasonably similar at relatively low pyrolysis temperatures (<408 °C, Figure 10a,d) but increased far more than calculated around the generation peak (420 °C). Taken together, the measured yields for total C_{6+} hydrocarbons were first slightly lower than the calculated yields and became slightly larger than the calculated yields around the generation peak (420 °C, Figure 10c,f). When significant cracking occurred above 452 °C, the measured and calculated yields showed little difference.

A previously described mechanism[48] was adopted in this work to explain the differences discussed above, that is, preferential α-cleavage of the alkyl side-chain attached to the aromatic ring system and reincorporation of the corresponding radical into the aromatic ring system. At relatively low temperatures, long alkyl chains in the oil might have been reincorporated into the aromatic ring system of the mature kerogen, thus leading to the much lower measured amount of C_{15+} hydrocarbons than calculated for simple mixing (Figure 10b,e). Nevertheless, enhanced cracking of released C_{15+} hydrocarbons into C_{6-14} hydrocarbons in the presence of kerogen might be a plausible explanation for the difference. At relatively high temperatures, the incorporated long chains could be released and might subsequently be cracked into shorter alkyl chains (C_{6-14}), as catalyzed by the kerogen. The result could be a larger amount of C_{6-14} hydrocarbons (Figure 8a,d) but could produce a smaller amount of C_{15+} hydrocarbons (Figure 10b,e) than that calculated for the simple mixing model.

4.3. Overall Effects of Oil Expulsion on Petroleum Potential. To better illustrate the overall petroleum potential of deep source rocks, it still remained necessary to explore the observed variations in the hydrocarbon fractions and in their combinations with oil-expulsion levels. Therefore, the maximum yields of the individual hydrocarbon fractions (C_{1-5}, C_{6-14}, C_{15+}), liquid hydrocarbons (C_{6+}), and total hydrocarbons (C_{1+}) from the oil−kerogen mixtures were analyzed further to examine their relationships with the oil-expulsion levels.

As such, the percentage of organic carbon of expellable "oil a" ($C_{oil\ a}$ %) in a specific mixture of "oil a" and mature kerogen was adopted rather than OEE values because the OEE value reflected only the percentage of expelled oil in total oil. This value was calculated as follows

https://dx.doi.org/10.1021/acs.energyfuels.0c00553
Energy Fuels 2020, 34, 9262−9274

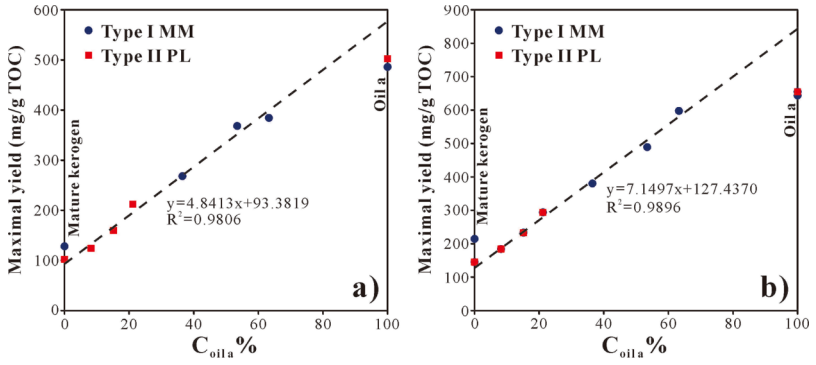

Figure 12. Relationships between $C_{oil\ a}$ % and maximum yields of (a) C_{6+} and (b) total hydrocarbons. Sample points plotted on the left- and right-hand *y*-axes represent mature kerogen and "oil a", respectively, and points lying between them represent their mixtures (linear regressions are determined using data for the mixture series only).

$$C_{oil\ a}\ \% = 100 \times [M_{oil\ a} \times TOC_{oil\ a} / (M_{oil\ a} \times TOC_{oil\ a} + M_{mature\ kerogen} \times TOC_{mature\ kerogen})]$$

Therefore, the $C_{oil\ a}$ % values for mature kerogen and expellable "oil a" were 0 and 100, respectively (Figure 11). The maximum yields of individual hydrocarbon fractions were found to be linearly correlated with $C_{oil\ a}$ % only for mature kerogen and the corresponding mixtures (Figure 11), and their yields from "oil a" generally deviated appreciably from the regression lines (both lower and higher), which was consistent with the different and complex influences of kerogen on oil cracking exemplified in the previous section (Figures 9 and 10). In addition, the trend of total gas yields showed large differences for type I MM and type II PL kerogens (Figure 11a). The two regression lines for the yields of C_{15+} were clearly different, primarily in terms of the larger intercept (by ~20 mg/g TOC, Figure 11c). In contrast, the trend of C_{6-14} yields defined by type I MM kerogens was almost the same as that defined by type II PL kerogens (Figure 11b). This observation suggested that the C_{6-14} potential from source rocks containing type I/II mature kerogens could be determined if the amount of expellable "oil a" with respect to immature kerogen were known. However, one should recall the dependence of this amount on the composition of the solvent used in extraction. Clear differences in the yield trends of total gases and C_{15+} for types I and II kerogens were related more closely to the larger hydrocarbon yields of type I mature kerogen than type II (Figure 11a,c), although the C_{6-14} yields were almost identical for the two mature kerogens (Figure 11b).

Following the above idea, the yields of total liquid hydrocarbons (C_{6+}) and total hydrocarbons (C_{1+}) were further analyzed (Figure 12). However, regression analysis was performed only on the combined data for the mixtures, and data for both mature kerogen and "oil a" were excluded. The regression line, if the maximum yield for type I and II mature kerogens were included, showed only notably slight changes in both slope (4.7677) and intercept (96.7079) compared with the regression line in Figure 12a. For total hydrocarbons (Figure 12b), the slope was 6.9980 and the intercept was 134.2959, also without significant variations. These values demonstrated an overall mass balance for cracking from oil to total hydrocarbons (C_{1+}) and for cracking from heavy hydrocarbons (C_{15+}) to light hydrocarbons (C_{6-14}). Therefore, the formulas might offer an approximate method of estimating the petroleum potential of source rocks after the main oil generation and expulsion.

5. CONCLUSIONS

Oil expulsion was simulated using the proposed new approach of selective solvent extraction to show the differences in both the amount and composition of expellable "oil a" from distinct types of mature kerogen. Further oil migration from shale was quantitatively performed by adding back "oil a" to the mature kerogen in controlled mass ratios. In this manner, the light oil and condensate potentials from deep source rocks were investigated by measuring the yields of gas, C_{6+}, and C_{6-14} hydrocarbons from the mature kerogen together with its admixed "oil a". The main conclusions are given as follows:

1. The GOR of pyrolyzates was used to determine the maturity range for the light oil, condensate and gas stages. The lowest EVR_o that was determined for the gas stage (1.9−2.1%) was consistent with the EVR_o value used in commonly accepted models. The light oil/condensate cutoff EVR_o was found to be approximately 1.55−1.75%, which was higher than that of the traditional models. This result was largely related to the question of whether a general or rigorous definition of "condensate" was adopted. The EVR_o range from 1.35 to 1.55−1.75% was defined in this work as a "light oil/gas" substage within the usual definition of "condensate/wet gas".

2. The yields of the individual hydrocarbon fractions from "oil a" cracking were clearly affected by the presence of mature kerogens. This effect showed little difference between type I and type II kerogens on the yield of C_{6-14} hydrocarbons and a slightly different yield of C_{15+} hydrocarbons but a significant difference in gas yield. For liquid hydrocarbons, the release of C_{15+} from "oil a" cracking was inhibited but was promoted for C_{6-14} hydrocarbons. These results were attributed to reincorporation of the long alkyl chains into relatively low-maturity kerogen structures, which were subsequently released and quickly cracked into shorter alkyl chains (C_{6-14}) catalyzed by relatively high-maturity kerogen. The influence on gas yields from "oil a" cracking was complex and was related to the kerogen type. Total gas yields from oil cracking were promoted at the early cracking stage only by mature type II kerogen but were not significantly affected at the late stage because of the enhanced production of methane. However, the release of gases at the late cracking stages was clearly inhibited for type I kerogen.

3. Despite these complicated effects on yield, approximately linear relationships were nevertheless established between the

https://dx.doi.org/10.1021/acs.energyfuels.0c00553
Energy Fuels 2020, 34, 9262−9274

maximum yield of liquids (or total hydrocarbons) and the carbon content of "oil a" in its mixtures with mature kerogen. This result was possibly due to the compensation effects of generation and cracking of multiple hydrocarbon fractions. If so, the established relationships could aid in the estimation of the oil and total petroleum potential of deep source rocks that have undergone oil generation and expulsion. However, such a method is expected to certainly depend on the total and residual amount of expellable "oil a" in source rocks, and these factors were definitely affected by the solvents used in extraction..

■ ASSOCIATED CONTENT

Supporting Information

The Supporting Information is available free of charge at https://pubs.acs.org/doi/10.1021/acs.energyfuels.0c00553.

Yields of gases and C_{6+} and C_{6-14} fractions obtained at a heating rate of 2 °C/h (XLSX)

■ AUTHOR INFORMATION

Corresponding Author

Wanglu Jia − *State Key Laboratory of Organic Geochemistry, Guangzhou Institute of Geochemistry, Chinese Academy of Sciences, Guangzhou 510640, China;* orcid.org/0000-0003-1715-4279; Phone: +86-20-85291312; Email: wljia@gig.ac.cn; Fax: +86-20-85290706

Authors

Qiang Wang − *State Key Laboratory of Organic Geochemistry, Guangzhou Institute of Geochemistry, Chinese Academy of Sciences, Guangzhou 510640, China; University of Chinese Academy of Sciences, Beijing 100049, China*

Chiling Yu − *State Key Laboratory of Organic Geochemistry, Guangzhou Institute of Geochemistry, Chinese Academy of Sciences, Guangzhou 510640, China*

Jianzhong Song − *State Key Laboratory of Organic Geochemistry, Guangzhou Institute of Geochemistry, Chinese Academy of Sciences, Guangzhou 510640, China;* orcid.org/0000-0002-4467-4483

Hui Zhang − *State Key Laboratory of Organic Geochemistry, Guangzhou Institute of Geochemistry, Chinese Academy of Sciences, Guangzhou 510640, China; Changqing Oilfield Company, PetroChina, Xi'an 710018, China*

Jinzhong Liu − *State Key Laboratory of Organic Geochemistry, Guangzhou Institute of Geochemistry, Chinese Academy of Sciences, Guangzhou 510640, China*

Ping'an Peng − *State Key Laboratory of Organic Geochemistry, Guangzhou Institute of Geochemistry, Chinese Academy of Sciences, Guangzhou 510640, China; University of Chinese Academy of Sciences, Beijing 100049, China*

Complete contact information is available at: https://pubs.acs.org/10.1021/acs.energyfuels.0c00553

Notes

The authors declare no competing financial interest.

■ ACKNOWLEDGMENTS

This work was supported by the National Oil and Gas Major Project (2017ZX05008-002-010), the Strategic Priority Research Program (XDB10010201), the National Natural Science Foundation of China (41621062), and the State Key Laboratory of Organic Geochemistry (SKLOG2020-1). Two anonymous reviewers are gratefully acknowledged for their critical comments, which greatly improved the manuscript. We thank Dr. Ryan P. Rodgers for handling the manuscript.

■ REFERENCES

(1) EIA (Energy Information Administration, U.S.). The API gravity of crude oil produced in the U.S. varies widely across states. 2017, https://www.eia.gov/todayinenergy/detail.php?id=30852 (accesssed April 19, 2017).

(2) Cardott, B. J. Thermal maturity of Woodford shale gas and oil plays, Oklahoma, USA. *Int. J. Coal Geol.* **2012**, *103*, 109−119.

(3) Arouri, K. R.; Jenden, P. D.; Al-Hajji, A. A. Petroleum inclusions atop Unayzah gas condensate reservoir: Signpost for an undocumented chapter of the Arabian Basin filling history? *Org. Geochem.* **2010**, *41*, 698−705.

(4) Mobarakabad, A. F.; Bechtel, A.; Gratzer, R.; Mohsenian, E.; Sachsenhofer, R. F. Geochemistry and origin of crude oils and condensates from the central Persian gulf, offshore Iran. *J. Pet. Geol.* **2011**, *34*, 261−275.

(5) Huang, S.; Wang, Z.; Lv, Z.; Gong, D.; Yu, C.; Wu, W. Geochemical identification of marine and terrigenous condensates—a case study from the Sichuan Basin, SW China. *Org. Geochem.* **2014**, *74*, 44−58.

(6) Zhu, G.; Wang, H.; Weng, N.; Yang, H.; Zhang, K.; Liao, F.; Neng, Y. Geochemistry, origin and accumulation of continental condensate in the ultra-deep-buried cretaceous sandstone reservoir, kuqa depression, tarim basin, china. *Mar. Pet. Geol.* **2015**, *65*, 103−113.

(7) Mei, M.; Bissada, K. K.; Malloy, T. B.; Darnell, L. M.; Liu, Z.; Liu, Z. Origin of condensates and natural gases in the Almond Formation reservoirs in southwestern Wyoming, USA. *Org. Geochem.* **2018**, *124*, 164−179.

(8) Yang, H.; Zhu, G. The condensate gas field geological characteristics and its formation mechanism in Tarim basin. *Acta Petrol. Sin.* **2013**, *29*, 3233−3250.

(9) Chen, J.; Deng, C.; Wang, X.; Ni, Y.; Sun, Y.; Zhao, Z.; Liao, J.; Wang, P.; Zhang, D.; Liang, D. Formation mechanism of condensates, waxy and heavy oils in the southern margin of Junggar Basin, NW China. *Sci. China: Earth Sci.* **2017**, *60*, 972−991.

(10) Xu, C.; Yu, H.; Wang, J.; Liu, X. Formation conditions and accumulation characteristics of Bozhong 19-6 large condensate gas field in offshore Bohai Bay Basin. *Pet. Explor. Dev.* **2019**, *46*, 27−40.

(11) Montgomery, S. L.; Jarvie, D. M.; Bowker, K. A.; Pollastro, R. M. Mississippian Barnett shale, Fort Worth Basin, north-central Texas: Gas-shale play with multi-trillion cubic foot potential. *AAPG Bull.* **2005**, *89*, 155−175.

(12) Hao, F.; Zou, H.; Lu, Y. Mechanisms of shale gas storage: Implications for shale gas exploration in China. *AAPG Bull.* **2011**, *97*, 1325−1346.

(13) Tissot, B. P.; Welte, D. H. *Petroleum Formation and Occurrence*, 2nd ed.; Springer-Verlag: Berlin 1984.

(14) Peters, K. E.; Kacewicz, M.; Curry, D. J. An overview of basin and petroleum system modeling: Definitions and concepts. *Basin Modeling: New Horizons in Research and Applications*; AAPG, 2012; Vol. *4*, pp 1−16.

(15) Waples, D. W. The kinetics of in-reservoir oil destruction and gas formation: constraints from experimental and empirical data, and from thermodynamics. *Org. Geochem.* **2000**, *31*, 553−575.

(16) Schimmelmann, A.; Sessions, A. L.; Mastalerz, M. Hydrogen isotopic (D/H) composition of organic matter during diagenesis and thermal maturation. *Annu. Rev. Earth Planet. Sci.* **2006**, *34*, 501−533.

(17) Hill, R. J.; Zhang, E.; Katz, B. J.; Tang, Y. Modeling of gas generation from the Barnett Shale, Fort Worth Basin, Texas. *AAPG Bull.* **2007**, *91*, 501−521.

(18) Behar, F.; Jarvie, D. M. Compositional modeling of gas generation from two shale gas resource systems: Barnett shale (United States) and Posidonia shale (Germany). *AAPG Mem.* **2013**, *103*, 25−44.

(19) Jia, W.; Wang, Q.; Liu, J.; Peng, P. a.; Li, B.; Lu, J. The effect of oil expulsion or retention on further thermal degradation of kerogen at the high maturity stage: A pyrolysis study of type II kerogen from Pingliang shale. *Org. Geochem.* **2014**, *71*, 17−29.
(20) Gai, H.; Xiao, X.; Cheng, P.; Tian, H.; Fu, J. Gas generation of shale organic matter with different contents of residual oil based on a pyrolysis experiment. *Org. Geochem.* **2015**, *78*, 69−78.
(21) Gai, H.; Tian, H.; Xiao, X. Late gas generation potential for different types of shale source rocks: implications from pyrolysis experiments. *Int. J. Coal Geol.* **2018**, *193*, 16−29.
(22) Ritter, U. Solubility of petroleum compounds in kerogen: implications for petroleum expulsion. *Org. Geochem.* **2003**, *34*, 319−326.
(23) Jin, X.; Li, E.; Pan, C.; Yu, S.; Liu, J. Interaction of coal and oil in confined pyrolysis experiments: Insight from the yield and composition of gas hydrocarbons. *Mar. Pet. Geol.* **2013**, *48*, 379−391.
(24) Li, E.; Pan, C.; Yu, S.; Jin, X.; Liu, J. Interaction of coal and oil in confined pyrolysis experiments: Insight from the yields and carbon isotopes of gas and liquid hydrocarbons. *Mar. Pet. Geol.* **2016**, *69*, 13−37.
(25) Mahlstedt, N.; Horsfield, B. Metagenetic methane generation in gas shales I. Screening protocols using immature samples. *Mar. Pet. Geol.* **2012**, *31*, 27−42.
(26) Alcantar-Lopez, L. Understanding organic matter Structural changes with increasing thermal maturity from oil shale plays through SEM imaging. *Unconventional Resources Technology Conference*, 2016, URTeC control ID number 2456170.
(27) Pommer, M.; Milliken, K. Pore types and pore-size distributions across thermal maturity, Eagle Ford Formation, southern Texas. *AAPG Bull.* **2015**, *99*, 1713−1744.
(28) Loucks, R. G.; Reed, R. M. Scanning-electron-microscope petrographic evidence for distinguishing organic matter pores associated with depositional organic matter versus migrated organic matter in mudrocks. *Gulf Coast Assoc. Geol. Soc.* **2014**, *3*, 51−60.
(29) Behar, F.; Vandenbroucke, M.; Tang, Y.; Marquis, F.; Espitalie, J. Thermal cracking of kerogen in open and closed systems: determination of kinetic parameters and stoichiometric coefficients for oil and gas generation. *Org. Geochem.* **1997**, *26*, 321−339.
(30) Kelemen, S. R.; Afeworki, M.; Gorbaty, M. L.; Sansone, M.; Kwiatek, P. J.; Walters, C. C.; Freund, H.; Siskin, M.; Bence, A. E.; Curry, D. J.; Solum, M.; Pugmire, R. J.; Vandenbroucke, M.; Leblond, M.; Behar, F. Direct Characterization of kerogen by X-ray and solid-State ^{13}C nuclear magnetic resonance methods. *Energy Fuels* **2007**, *21*, 1548−1561.
(31) Ungerer, P.; Collell, J.; Yiannourakou, M. Molecular modeling of the volumetric and thermodynamic properties of kerogen: Influence of organic type and maturity. *Energy Fuels* **2015**, *29*, 91−105.
(32) Bai, H.; Pang, X.; Kuang, L.; Pang, H.; Wang, X.; Jia, X.; Zhou, L.; Hu, T. Hydrocarbon expulsion potential of source rocks and its influence on the distribution of lacustrine tight oil reservoir, Middle Permian Lucaogou Formation, Jimsar Sag, Junggar Basin, Northwest China. *J. Pet. Sci. Eng.* **2017**, *149*, 740−755.
(33) Hu, S.; Li, S.; Xia, L.; Lv, Q.; Cao, J. On the internal oil migration in shale systems and implications for shale oil accumulation: A combined petrological and geochemical investigation in the Eocene Nanxiang Basin, China. *J. Pet. Sci. Eng.* **2020**, *184*, 106493.
(34) Dembicki, H. Three common source rock evaluation errors made by geologists during prospect or play appraisals. *AAPG Bull.* **2009**, *93*, 341−356.
(35) Pepper, A. S.; Corvi, P. J. Simple kinetic models of petroleum formation. Part III: Modelling an open system. *Mar. Pet. Geol.* **1995**, *12*, 417−452.
(36) Pan, C.; Jiang, L.; Liu, J.; Zhang, S.; Zhu, G. The effects of calcite and montmorillonite on oil cracking in confined pyrolysis experiments. *Org. Geochem.* **2010**, *41*, 611−626.
(37) Tian, H.; Xiao, X.; Wilkins, R. W. T.; Gan, H.; Guo, L.; Yang, L. Genetic origins of marine gases in the Tazhong area of the Tarim basin, NW China: Implications from the pyrolysis of marine kerogens and crude oil. *Int. J. Coal Geol.* **2010**, *82*, 17−26.
(38) Tian, H.; Xiao, X.; Wilkins, R. W. T.; Tang, Y. An experimental comparison of gas generation from three oil fractions: Implications for the chemical and stable carbon isotopic signatures of oil cracking gas. *Org. Geochem.* **2012**, *46*, 96−112.
(39) Lorant, F.; Behar, F. Late generation of methane from mature kerogens. *Energy Fuels* **2002**, *16*, 412−427.
(40) Hill, R. J.; Tang, Y.; Kaplan, I. R. Insights into oil cracking based on laboratory experiments. *Org. Geochem.* **2003**, *34*, 1651−1672.
(41) Behar, F.; Pelet, R.; Roucache, J. Geochemistry of asphaltenes. *Org. Geochem.* **1984**, *6*, 587−595.
(42) Bowden, S. A.; Farrimond, P.; Snape, C. E.; Love, G. D. Compositional differences in biomarker constituents of the hydrocarbon, resin, asphaltene and kerogen fractions: an example from the Jet Rock (Yorkshire, UK). *Org. Geochem.* **2006**, *37*, 369−383.
(43) Behar, F.; Kressmann, S.; Rudkiewicz, J. L.; Vandenbroucke, M. Experimental simulation in a confined system and kinetic modelling of kerogen and oil cracking. *Org. Geochem.* **1992**, *19*, 173−189.
(44) Dieckmann, V.; Schenk, H. J.; Horsfield, B.; Welte, D. H. Kinetics of petroleum generation and cracking by programmed-temperature closed-system pyrolysis of Toarcian Shales. *Fuel* **1998**, *77*, 23−31.
(45) Boyd, D. T. *Oklahoma's Oil and Gas Industry and the Global Forces Controlling It*; Oklahoma City Geological Society Shale Shaker, 2006; Vol. *56*, pp 145−154.
(46) Sweeney, J. J.; Burnham, A. K. Evaluation of a simple model of vitrinite reflectance based on chemical kinetics. *AAPG Bull.* **1990**, *74*, 1559−1570.
(47) Zhang, H. Suppression of vitrinite reflectance, apatite fission track analysis and the recovery of original organic carbon abundance for high-mature kerogen: Kinetic approaches. Ph.D. Thesis, Guangzhou Institute of Geochemistry, Chinese Academy of Sciences, 2008.
(48) McNeil, R. I.; Bement, W. O. Thermal stability of hydrocarbons: Laboratory criteria and field examples. *Energy Fuels* **1996**, *10*, 60−67.

https://dx.doi.org/10.1021/acs.energyfuels.0c00553
Energy Fuels 2020, 34, 9262−9274